Fermi National Accelerator Laboratory

FERMILAB-Pub-87/26
0102.000
0103.000

# Advanced Accelerator Concepts and Electron-Positron Linear Colliders*

R.H. Siemann
Fermi National Accelerator Laboratory
P.O. Box 500, Batavia, Illinois 60510

and

Newman Laboratory of Nuclear Studies, Cornell University**
Ithaca, New York 14853

January 1987

*(Submitted to Annual Review of Nuclear and Particle Science)
**Permanent Address

Operated by Universities Research Association Inc. under contract with the United States Department of Energy

# ADVANCED ACCELERATOR CONCEPTS AND ELECTRON-POSITRON LINEAR COLLIDERS

R. H. Siemann

Accelerator Division, Fermi National Accelerator Laboratory,
Batavia, Illinois 60510*

and

Newman Laboratory of Nuclear Studies, Cornell University,
Ithaca, New York 14853**

(Submitted to Annual Review of Nuclear and Particle Science)

CONTENTS



* Operated by Universities Research Association, Inc under contract with the United States Department of Energy

** Permanent address

## INTRODUCTION

Many high energy physics phenomena can be understood through the Standard Model of elementary particles and their interactions. Key experiments in the development of this model were made possible through advances in accelerator physics: stochastic cooling led to the discovery of the $W^{\pm}$ and $Z^{o}$ intermediate bosons, and electron-positron storage ring development led to the discovery of the $\tau$ lepton and one of the two independent discoveries of the $J/\psi$. While the Standard Model has been extremely successful, phenomena including the quark and lepton mass spectra and the symmetry breaking mechanism in the electroweak theory are not encompassed. Experiments at the TeV mass scale should give important information about these questions.

Either a linear or a storage ring collider must be used to reach these high energies. There is substantial experience with storage rings, and they are feasible for multi-TeV proton beams. The Superconducting Super Collider design (1) has shown that the accelerator physics considerations for such a ring are not qualitatively different from those of the past. For electron beams, storage rings are inconceivable because of large synchrotron radiation energy losses, and, as a result, linear colliders are the only possible technique. Although the linear collider concept (2, 3) was introduced in 1965, the Stanford Linear Collider (4; SLC), which has a beam energy of 50 GeV and is expected to become operational in 1987, is the first of this class of accelerator. At present, linear colliders do not have the experience base of storage rings. In addition, from the arguments detailed in the next section, technological developments beyond the SLC are needed for a TeV energy linear collider.

Given the sharp contrast between the need for these developments and the present feasibility of a proton storage ring, why pursue the novel acceleration techniques needed for linear colliders? There are two clear reasons. First, energy is not the only parameter of importance for experiments. Electron-positron colliders have proven superior for many types of experiments because of the well-determined quantum numbers of the initial state and low backgrounds. Therefore, a scientific case for an electron-positron collider covering the same mass range as a proton collider may develop. Second, the resultant technology may allow us to reach even higher energies than possible with proton storage rings. For these reasons there is substantial interest in novel acceleration techniques, and, just as in the past, advances in accelerator physics may be key to our understanding of nature.

## SCALING LAWS FOR $e^+e^-$ LINEAR COLLIDERS

The requirements of high energy physics together with economic arguments lead to general relationships which are independent of specific acceleration mechanisms. Center-of-mass energy and luminosity are the primary high energy physics parameters. The cross section for the production of muon pairs sets the scale of interesting luminosities. At 2 TeV center-of-mass energy and a luminosity of $10^{33}$ $cm^{-2}sec^{-1}$ the event rate for $e^+e^- \rightarrow \mu^+\mu^-$ is 0.9 events per day. Luminosities greater than $10^{33}$ $cm^{-2}sec^{-1}$ are welcome!

Considerations of capital and operating costs are having substantial impact on the development of novel accelerator concepts. Estimates of capital costs are unreliable as most concepts are at a "proof-of-principle" stage, but a cost scaling analysis performed by Palmer (5) gives general guidance to cost effective parameters. This analysis relates most closely to radio frequency driven accelerators, and a similar discussion will be presented in the section on near-field accelerators. The beam power and the efficiency for conversion of "wall-plug" power to beam power determine the operating cost. While the conversion efficiency must be considered separately for different acceleration mechanisms, there is a direct trade-off between beam power and beam quality. This trade-off follows from the scaling laws developed below.

In terms of accelerator parameters the luminosity is given by (6)

$$L = \frac{N^2 \, f \, H_D}{4 \pi \sigma_x \sigma_y} \qquad 1.$$

where N is the number of particles per beam bunch (assumed to be equal for the two beams), f is collision frequency, $H_D$ is a luminosity enhancement factor caused by "disruption", and $\sigma_x$ and $\sigma_y$ are the rms beam sizes in the horizontal and vertical respectively. In addition to the hard collisions which produce elementary particles, the beams interact through their electromagnetic fields. This interaction is the dominant influence on beam behavior. It leads to beam focusing which is called "disruption" and photon radiation which is named "beamstrahlung", a name intended to evoke images of bremsstrahlung.

Disruption is characterized by a disruption parameter which measures the strength of the focusing provided by the oncoming beam. For small values of the disruption parameter there is an enhancement of luminosity, given by $H_D$, due to this focusing. At large values, particles undergo transverse plasma oscillations, a situation which is almost certainly unstable and to be avoided. Reasonable values for $H_D$ are thought to be between one and five (7, 8).

Beamstrahlung lowers the average center-of-mass energy and introduces a spread in this energy. The average energy loss has been calculated in two regimes: the "classical" regime (9) where the radiation spectrum is that of synchrotron radiation with the critical energy much less than the beam energy, and the "quantum" regime (10)[1] where the critical energy is much greater than the beam energy and, as a result, the spectrum is cut-off at the beam energy. These calculations give beamstrahlung parameters, $\delta_{cl}$ and $\delta_q$, which are the average fractional energy losses and have different dependences on bunch dimensions, number of particles, and beam energy (6). In addition, the distribution of center-of-mass energies is different in the two regimes.

Expressions for the luminosity, beam power $P_b$, and the beamstrahlung parameters can be combined to give scaling relationships for linear

1 R. Blankenbeckler and S. Drell are studying the validity of the quantum beamstrahlung calculation at short bunch lengths; their results could affect Equation 3.

colliders in the classical and quantum regimes (6):

$$\frac{L^2 \gamma^3}{\delta_{cl}} = 7.2 \times 10^{-3} \frac{(\sigma_x + \sigma_y)^2 \sigma_z H_D P_b^2}{r_e^3 (m_e c^2)^2 \sigma_x^2 \sigma_y^2} , \qquad 2.$$

and

$$\frac{L^2 \gamma}{\delta_q^3} = 0.05 \frac{H_D (\sigma_x + \sigma_y)^2 P_b^2}{\alpha^4 r_e (m_e c^2)^2 \sigma_x^2 \sigma_y^2 \sigma_z} . \qquad 3.$$

$\alpha$, $r_e$, and $m_e c^2$ are the fine structure constant, the classical radius of the electron, and the rest energy of the electron; $\gamma$ is the beam energy in units of rest energy, and $\sigma_z$ is the rms bunch length. The parameters on the left-hand sides are determined by particle physics requirements, and once these are fixed the scaling laws relate beam power and beam dimensions.

Equations 2 and 3 are plotted in Figure 1 which shows several important features of these equations. First, since most novel acceleration techniques employ short bunches, it is probable that a very high energy collider would operate in the quantum regime. The transition from the classical to the quantum regime occurs at shorter bunch lengths as the energy decreases, and, as a result, a lower energy collider using the same acceleration method may operate in a different beamstrahlung regime. Second, the beam radius is extremely small and directly proportional to the beam power and operating cost. Low beam power requires a small radius and, equivalently, good beam quality. Preservation of beam quality during acceleration is a critical issue discussed in more detail in the next section.

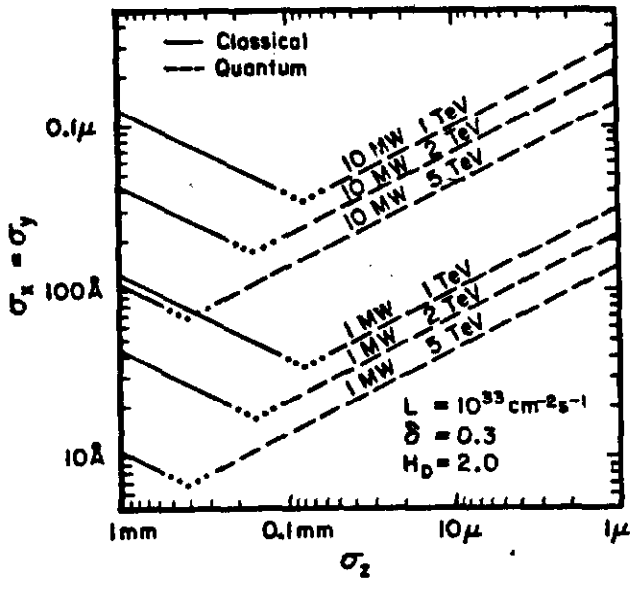


Figure 1: Linear collider scaling laws in the classical and quantum regimes assuming a round beam. Beamstrahlung is in the classical (quantum) regime at large (small) $\sigma_z$.

## BEAM QUALITY AND WAKEFIELDS

The acceleration and focusing of a particle can be described by a trajectory in six-dimensional phase space[2]. Liouville's theorem states that the phase-space density about any such trajectory is constant, and, consequently, the phase-space volume of the beam is constant although its shape may change. However, a distinction must be drawn between this statement and a more practical point-of-view. A beam may develop a complicated, filament-like structure enclosing empty regions of phase space. Theoretically, the phase-space filaments can be untangled, but this is impractical, and the average density of the beam has become lower. For a given intensity the useful measures of beam quality are the emittances which are the projections of the occupied volume onto $(x,p_x)$, $(y,p_y)$, and $(z,p_z)$ planes. These emittances are constant at best.

In each of the transverse dimensions the spot size ($\sigma_x$, $\sigma_y$) and the angular divergence ($\sigma_x'$, $\sigma_y'$) at the collision point are related to the emittance ($\epsilon_x$, $\epsilon_y$) by

$$\sigma_i \, \sigma_i' = \frac{\epsilon_i}{\gamma \, m_o \, c^2} ; \quad i = x, \, y \, . \qquad 4.$$

Focusing the beam to a small spot demands a strong final lens, and a common feature of ideas for making such a lens (11, 12; R. B. Palmer private communication) is a small beam size at the lens or equivalently a small angular divergence at the collision point. The combination of a small spot and a strong final lens call for small transverse emittances; for the spot sizes in Figure 1, these emittances need to be several orders of magnitude smaller than obtained to date.

The longitudinal emittance is the product of energy spread and bunch length. For a small collision spot the chromatic and geometric aberrations of the interaction region optical system need to be corrected to high order. These corrections are difficult (13), and they place an upper limit on the energy spread. This limit combined with the short bunch length required to operate in the quantum beamstrahlung regime calls for a small longitudinal emittance.

Beam generated electromagnetic fields called "wakefields" tend to increase the beam emittances. Figure 2a, the result of a computer simulation of beam behavior in the SLC (14), presents a graphic example. In this simulation the beam is injected with a 30 $\mu$m position error (with respect to the symmetry axis of the structure). As a result of this displacement deflecting wakefields are generated. After acceleration, trailing particles have a large transverse displacement, and the transverse emittance has increased. Transverse emittance growth can also be initiated by misalignment of accelerator sections or focusing elements (6). Ways to prevent this are:

1. Removing misalignments and injection errors;
2. Using strong focusing along the accelerator;

---

2 The phase-space coordinates are the three spatial coordinates and their conjugate momenta.

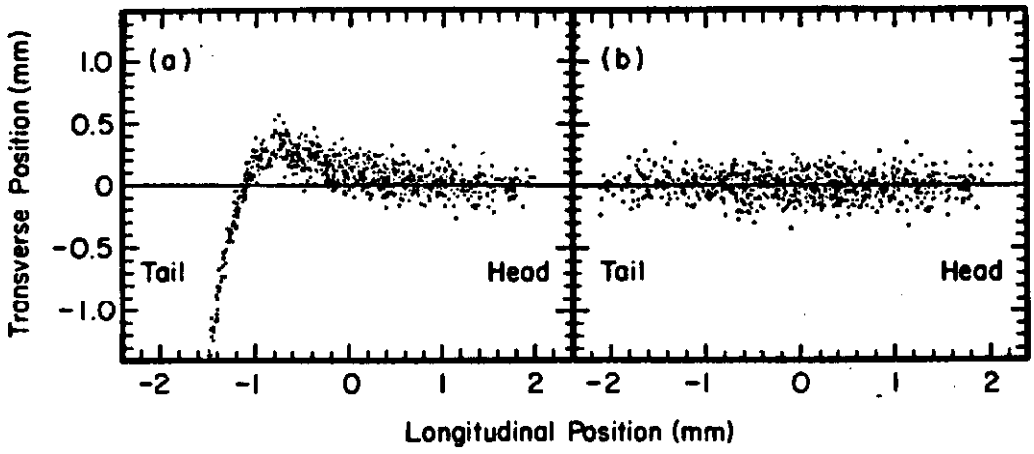


Figure 2: The results of a simulation of beam behavior in the SLC (14). In obtaining Figure 2b Landau damping was used to prevent emittance blow-up. (Reprinted with permission of K. L. F. Bane)

3. Using Landau damping (14, 15). If the beam particles have a spread in focusing strength (with quadrupole magnets this will be directly proportional to the beam energy spread) they do not move in phase, and the emittance blow-up is strongly damped as shown in Figure 2b.
4. Choosing an accelerator with small wakefields.

The example in Figure 2 shows the effect of transverse wakefields. There are also longitudinal wakefields which have only a decelerating component[3]. These lead to an energy spread which is roughly inversely proportional to the bunch length. The longitudinal emittance, $\sigma_\gamma \sigma_z$, is determined by the accelerator structure and can be reduced by the choice of accelerator (the fourth method above). The interplay between wakefields and accelerator properties is expanded in the next section.

NEAR-FIELD ACCELERATORS

An accelerating electromagnetic wave must have a phase velocity equal to the beam velocity and a component of electric field in the direction of propagation. These waves can propagate in a variety of structures with the common feature of a periodic substructure with size and period comparable to the wavelength. The importance of nearby boundaries leads to the general classification of "near-field" accelerators. The most familiar example is the radio-frequency (RF) driven, disk-loaded, cylindrical waveguide.

For electron linear accelerators most experience is with 10 cm wavelength (S-band), room temperature structures. It would be natural to think of a very high energy collider based on this experience, but considerations of beam power and efficiency argue against this. Since these structures have a group velocity much less than the speed of light, a section of accelerator is "filled" with electromagnetic energy before the beam arrives. The beam extracts a fraction of this energy, and that remaining must be thrown away or saved for subsequent beam pulses.

The electromagnetic field energy per unit length is proportional to the square of a typical transverse dimension and the square of a typical

3 The transverse (longitudinal) wakefield is the transverse momentum (energy) change per unit length of accelerator.

field. The waveguide dimensions scale as the wavelength of the fundamental mode $\lambda$, and the accelerating gradient G can be taken as a typical field. The energy extraction efficiency $\eta_b$ is

$$\eta_b = A_b \frac{N\,G}{\lambda^2\,G^2} = A_b \frac{N}{\lambda^2\,G} . \qquad 5.$$

The proportionality constant, $A_b$, is 13.4 x $10^{-8}$ V-m for the SLAC S-band linac (6).

The beam's fractional energy spread depends on $\eta_b$, $\sigma_z/\lambda$, and the phase of the bunch with respect to the accelerating wave. If the phase is chosen to minimize the energy spread,

$$\eta_b \propto \frac{\sigma_\gamma\,\sigma_z}{\gamma\,\lambda} . \qquad 6.$$

The proportionality constant depends on the structure (6). The choices for high efficiency are large longitudinal emittance, short wavelengths or saving RF energy for subsequent beam pulses.

Efficiency is one factor entering into a choice of wavelength; others are the dependence of limiting gradient on wavelength, transverse wakefields, and the availability of appropriate RF or laser power sources. The limitations on gradient from surface heating and electric field breakdown improve as the wavelength is reduced (6). However, with all other parameters fixed, the beam power is proportional to the gradient, and it may not be economical to operate near the limiting gradient.

Transverse wakefields favor long wavelengths. When $\lambda \gg \sigma_z$, the transverse wakefield within the bunch is linear with distance from the head. If the proportions of the accelerator are held fixed while the overall size is scaled to change the fundamental wavelength and the bunch length is kept a fixed fraction of the wavelength, the transverse wakefield at the tail varies as $\lambda^{-3}$ (6). For weaker dependence on $\lambda$, $\sigma_z/\lambda$ must be reduced at the cost of increasing the beam power and decreasing $\eta_b$. As mentioned earlier, transverse wakefield effects can be damped with Landau damping which comes from the energy spread of the beam. To the extent that Landau damping can be used the longitudinal emittance and $\eta_b$ can be increased. While a detailed parametric study is needed for quantitative results, it is clear that short wavelengths are not favored by transverse wakefield considerations.

Any choice of wavelength is strongly influenced by the availability of an appropriate power source. The average power and peak power requirements depend on wavelength as $\lambda^2$ and $\lambda^{1/2}$ respectively. The former follows directly from the stored energy and the latter from the stored energy and the decrease in structure filling time at short wavelengths (6). These requirements are formidable, and at almost all wavelengths power source development is needed. Ultimately, considerations of power sources, economy, wakefields, fabrication tolerances, etc. must be balanced in the design of an accelerator system. Since developments are still required before this can be done intelligently, a wide variety of approaches covering the wavelength range from $\lambda$ = 10 cm to $\lambda$ = 10 $\mu$m are under study. These are now described briefly.

Superconducting RF offers the advantage of being able to work at long wavelengths with a small number of continuous wave (CW) klystrons of proven design and a high efficiency for conversion of RF energy to beam energy. This high efficiency is obtained because the decay time of the RF energy would be much longer than the time between beam pulses, and many beam bunches can be accelerated per RF pulse. This remains possible even if sufficient time for damping wakefields between bunches is required because external couplers can damp modes other than the fundamental without affecting the Q of the fundamental mode (16).

To be practical for a high energy linear collider the gradient and fundamental mode Q must be increased from the presently obtained values of 5-10 MeV/m and 3-5 x $10^9$. There is a fundamental limit to the gradient from the magnetic field at the surface of the superconductor. For Nb this limit is roughly 50 Mev/m, and for $Nb_3Sn$ it is approximately 80 MeV/m (17). In the past five years there has been substantial progress with the solution of multipacting and material defect problems (18), and at present the gradient is limited by field emission. This is under active study (17).

The fundamental mode Q must be increased to make the cost of cooling the structure affordable. With the Q raised to 5 x $10^{10}$ and by operating with a modest duty cycle of 10-15% the cryogenic power requirements can be reduced to the range of several hundred megawatts which is beginning to become reasonable (19, 20).

In the design of a normal conducting linear accelerator there is a compromise between the peak power requirement and the structure efficiency defined as the inverse of the fraction of energy lost during the filling time. A factor of two increase above the minimum peak power increases the structure efficiency by about 2.5. Even with such an increase the average power at $\lambda$ = 10 cm is prohibitive, and for $\lambda$ = 3 cm it is acceptable only if multiple bunches can be accelerated with each RF pulse. It is unclear whether this is possible without interference between bunches due to wakefields. By reducing $\lambda$ to 1 cm it is possible to obtain reasonable efficiency with a single beam pulse per RF pulse (21). Small sections of a 1 cm wavelength disk-loaded waveguide have been constructed and tested (22); an average gradient of 180 MeV/m was produced. Future studies at this wavelength must include manufacturing tolerances, provision of water cooling, alignment and potentially critical effects of wakefields.

For some representative parameters (21) the peak power requirement is 25-100 MW per meter of accelerator structure. The research and development work aimed at meeting this demand falls into one of two general categories: microwave power tubes and "two-beam" devices. Consider the RF power tubes first.

Over 150 MW peak power has been obtained with good efficiency from a pulsed klystron at $\lambda$ = 10 cm (23). However, this design cannot be used in the 1-3 cm wavelength range because the peak power capability of any given design falls with wavelength as $\lambda^2$. This is a consequence of space charge limits on current density combining with decreasing cathode area to reduce the beam current (21). For high power at short wavelengths the beam current must be increased by employing a ring or sheet beam which would interact with an appropriate cavity mode. For

example, in the case of a hollow ring beam that mode is one with an electric field maximum at the beam radius. Preliminary work is beginning on the design of klystrons for these wavelengths employing ring and sheet current beams (24), but it is too early to have results.

The beam electrons in a gyroklystron undergo cyclotron motion and interact with a cavity TE mode. The cavities can be substantially larger than the wavelength, and as a result high beam currents used. A disadvantage of the gyroklystron is that the longitudinal component of the electron velocity must be kept large to counteract space charge forces, and the energy in this motion is not available for conversion into RF. As a result the efficiency is limited to between 30 and 40%. Work is well advanced on the design and construction of a $\lambda$ = 3 cm gyroklystron with a peak power output of 30 MW (25), and simulations are being used to study the scaling of this design up to 300 MW.

In the lasertron the cathode is a photoemitter, and by striking this cathode with RF modulated laser light the bunching cavities of the klystron are unneeded. Several experimental studies of the lasertron are underway (26, 27; J. LeDuff private communication). In the work being performed at SLAC (26), a lasertron for $\lambda$ = 10 cm with a peak output power of 35 MW and an efficiency of 70% is under development. In the future it is expected that power levels of roughly 100 MW can be reached with roughly the same efficiency. The usefulness of this concept for very high energy linear colliders will depend on the results of studies of scaling to smaller wavelengths. As with the klystron ring or sheet beam geometries could be used to obtain high power at short wavelengths.

Pulse compression schemes combine the power over a long pulse into a shorter, higher power pulse through the use of delay lines or energy storage cavities. These schemes can be important for increasing peak power or matching the pulse length of the tube to the accelerator fill time. An attractive idea for pulse compression, called Binary Pulse Compression (28), uses delay lines, hybrid junctions, and phase reversals at the (low) drive power level. The delay lines are low loss lines running in a TE mode, and it is expected that losses will be sufficiently small to allow multiplication of peak powers by a factor of sixteen or more. Experimental tests are underway.

With any approach based on tubes, thousands will be needed. This unappealing prospect is avoided in two-beam accelerators in which RF energy is extracted from the "drive beam", a low-energy, high-current beam traveling parallel to the high energy accelerator (see Figure 3). The RF energy is replaced by reaccelerating the drive beam. Two-beam accelerator concepts differ in the methods of energy extraction and reacceleration.

The original "Two-Beam Accelerator"[4] combined induction modules for acceleration with free electron lasers (FEL) for energy extraction (29). Induction modules offer efficient conversion of input power to beam power at a high repetition rate and moderate duty cycle (30). In the FEL section the beam oscillates transversely in the periodic magnetic

4 Andy Sessler, the inventor of this approach, coined the name "Two-Beam Accelerator" which still refers to this specific two-beam concept.

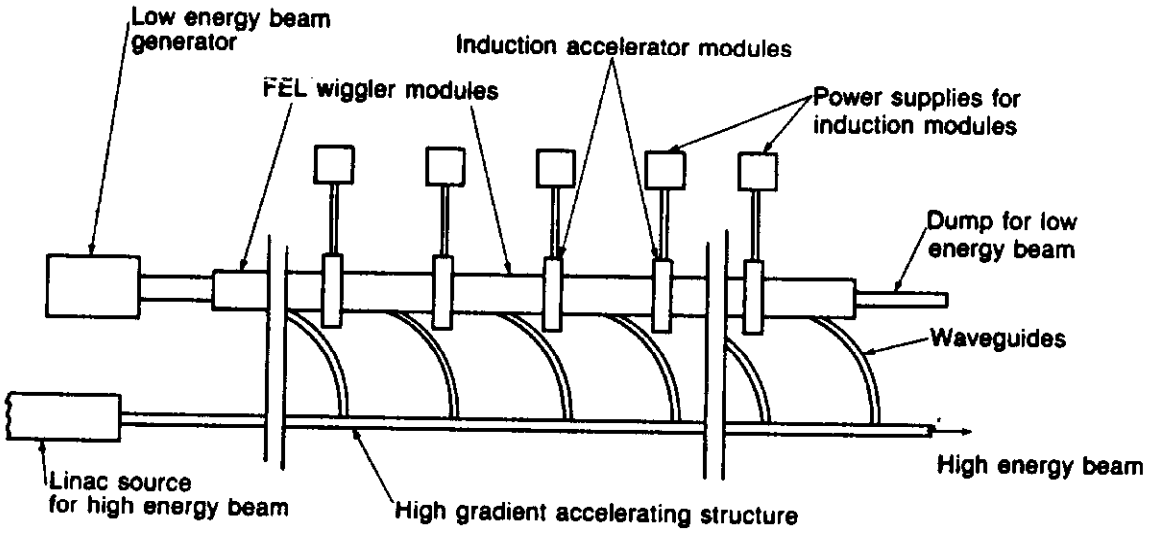


Figure 3: Schematic of the "Two-Beam Accelerator" (29). This figure illustrates one of several possible two-beam concepts which have the common features of a low energy drive beam running parallel to the high energy accelerator. (Reprinted with permission of A. Sessler)

field of a "wiggler" magnet. The wiggler wavelength is $\gamma^2$ times the radiation wavelength, and high efficiency is possible through use of a tapered wiggler, a wiggler in which the wavelength or magnetic field changes to compensate for decreasing beam energy as RF is radiated (31).

RF power generation with an FEL has been experimentally tested with impressive results (32): an energy extraction efficiency of 34% and a peak power greater than 1.0 GW at $\lambda$ = 8.7 mm. These results were obtained with a 3 m long tapered wiggler and a beam current and energy of 850 A and 3.5 MeV. Calculations and simulations studying other important aspects of this power source including reacceleration, FEL sidebands and long-term beam stability, phase jitter, and RF extraction are in progress with generally encouraging results (33). In addition, further experimental work including development of a prototype Two-Beam Accelerator is being planned.

A second two-beam approach combines superconducting RF for acceleration and bunched beam interaction with a resonant cavity, as in klystron, for energy extraction (34). The RF energy in the drive linac is supplied by large CW klystrons, and the drive beam pulses are short and spaced to match the repetition rate of the high energy accelerator. Superconducting RF allows efficient storage of energy between beam pulses; the required performance is that achieved routinely at present.

There are two other combinations of these acceleration and energy extraction methods: the "relativistic klystron" employing induction modules and klystron interaction (35), and a superconducting linac combined with an FEL (36). To date the optimal two-beam concept is not clear. Each concept has merits and drawbacks; for example, those with

superconducting RF have the advantage of higher repetition rate and the disadvantage of generation and stability of intense beams in a multi-cavity linear accelerator. In all cases calculations and simulations are incomplete, and experimental work has been performed on only one of four ideas.

It was thought that a disk-loaded waveguide for $\lambda \ll 1$ cm would be impractical to fabricate, and other conductor configurations with accelerating fields were considered. Predominantly these were "open" configurations with one or more sides missing to allow for easier fabrication and coupling of energy from power source to accelerator. One of the first laser accelerator ideas was that of an optical grating as a near-field accelerator (37). The general properties of open structures have been studied (38), and a number of innovative ideas including ink jets and etching have been suggested for accelerator construction. Small sections of accelerator have been made by etching, and as this technology has been understood, new ideas for structures have developed (39). Among them is a row of connected holes which resembles a disk-loaded waveguide.

Possible power sources for a short wavelength accelerator include FEL's, $CO_2$ lasers, and the "microlasertron". FEL's can operate at wavelengths as short as the ultraviolet, but there is a trade-off between extraction efficiency and gain which becomes more restrictive as the wavelength decreases (40). With the present rapid pace of FEL development, there should be substantially more experience with these power sources in the near future.

At $\lambda = 10$ $\mu$m it is natural to consider a $CO_2$ laser as the power source. This laser should have a high efficiency for conversion of wall-plug power to laser power, a high repetition rate equal to that of the accelerator, a pulse length in the picosecond range to match the accelerator filling time, and a favorable pulse extraction format. These have been achieved individually, but not simultaneously (41). The results of a kinetics calculation for a high efficiency laser illustrates possible performance: a 3 psec output pulse length, and an efficiency of 20% obtained by extracting sixteen pulses spaced by 50 nsec (such multiple pulse extraction needs demonstration) (41). The efficiency of a single pulse is unacceptably low, and either multiple beam bunches must be accelerated per laser pulse or output pulses combined with pulse compression. While the applicability to a full energy collider is unclear, a $CO_2$ laser will be the power source at an advanced accelerator test facility being planned by a collaboration between Brookhaven National Laboratory and Los Alamos National Laboratory (42). Many ideas related to short wavelength accelerators will be tested at this facility.

The microlasertron is an adaptation of the lasertron for 1 to 10 mm wavelength (43). A large number of small cavities are constructed by etching, and a photocathode is incorporated in each of these. Modulated laser light strikes these photocathodes producing power. Though an individual cavity is not capable of high power, the large number compensates and, in fact, is an advantage because one cavity powers only a short section of accelerator. In principle, the efficiency can be close to 100%, but a number of detailed questions need study before the efficiency which can be realized in practice is known.

In addition to structures and power sources, other aspects of short wavelength accelerators have been considered in the past and need study in the future. The efficient coupling of energy from the power source to the accelerator is an example where the solution is strongly dependent on the overall system. With the microlasertron this coupling arises naturally while with a laser optical configurations leading to coupling must be considered in more detail. Overall, there has been progress in the development of short wavelength near-field accelerators with innovative solutions to the problems of small size.

## WAKEFIELD AND SWITCHED POWER ACCELERATORS

Wakefields, which usually limit performance, can be exploited for acceleration - a beam passing through a section of accelerator excites electromagnetic fields, and a second beam, injected with an appropriate time delay, is accelerated by these fields. In contrast with two-beam accelerators both beams travel in the same structure. For two point bunches traveling on collinear paths, energy conservation and linear superposition are sufficient to calculate the stopping distance of the leading bunch, and the acceleration gradient seen by a particle in the trailing bunch (44). While there is a trade-off between gradient and stopping distance, the transformer ratio R is limited.

$$R = \frac{\text{Gradient x Stopping Distance}}{\gamma_1} = \frac{\Delta\gamma_2}{\gamma_1} \leq 2 - \frac{n_2}{n_1} \qquad 7.$$

where $n_1$ and $\gamma_1$ ($n_2$ and $\gamma_2$) are the number of particles and energy of the leading (trailing) bunch. I. e. in this simple case the maximum energy increase is $2\gamma_1$. This surprising result holds also for any rigid, symmetric drive bunch (44). For $R > 2$ either the two beams must be non-collinear, or the drive beam not symmetric or not rigid.

The DESY Wakefield Transformer (45, 46) shown in Figure 4 achieves a substantially better transformer ratio through the use of an annular driving beam coaxial to the trailing beam. For this configuration the transformer ratio is approximately $(r_b/r_a)^{1/2}$ where $r_a$ is the radius of the hole and $r_b$ the radius of the driving beam. There are potentially serious beam dynamics problems with the wakefield transformer. Azimuthal non-uniformity of the driving beam leads to transverse deflections of the accelerated beam, and the small hole, needed for a high transformer ratio, causes large wakefields in the accelerated beam itself. Simulations are being used to study these problems quantitatively (47).

An experimental test of the wakefield transformer is in progress (48). This experiment will serve as a proof-of-principle and for the identification of problems and directions for future research. The goals are a transformer ratio of about ten and a gradient in excess of 100 MeV/m over a length of 0.42 m. The annular drive beam has been generated and accelerated up to 6 MeV. There have been some problems with the azimuthal uniformity and intensity of this beam, and these are under study (49). Construction of the apparatus is scheduled to be complete by the end of 1986, and results are anticipated shortly thereafter.

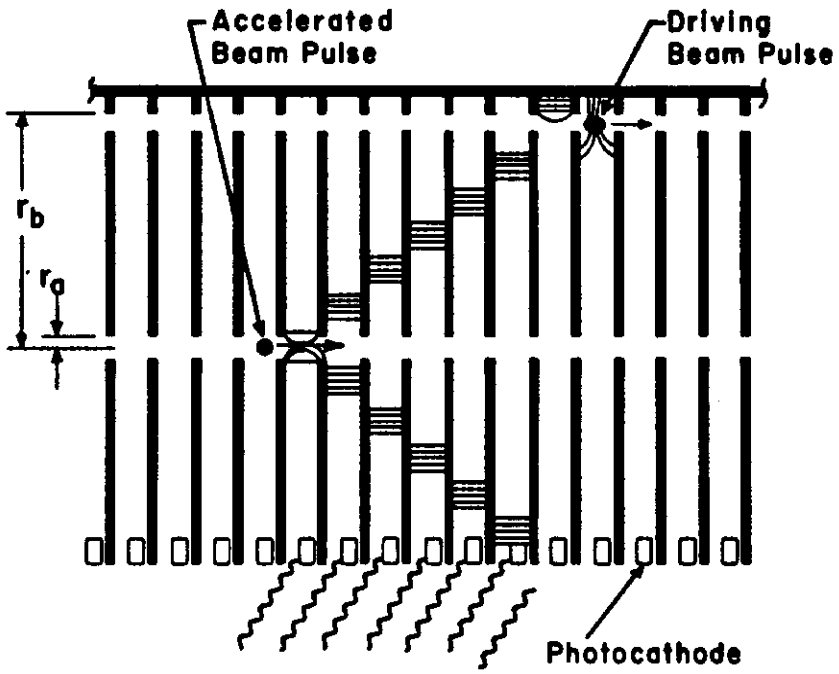


Figure 4: The DESY wakefield transformer (45, 46) and the switched power accelerator (53) are a set of disks illustrated in section view. Fields generated at $r_b$ (by either an annular beam or light striking annular photocathodes) propagate towards the center and accelerate the high energy beam.

The limit $R \leq 2$ holds for a rigid driving beam, a beam in which the relative longitudinal positions of particles do not change. Wakefields within a beam which is not ultra-relativistic can cause mixing, a change of relative position. The "wakeatron" uses a proton drive beam with a mixing distance short compared to the stopping distance and thereby achieves a transformer ratio above the limit (50). (Early wakefield acceleration schemes were based on a proton beam (51), but the transformer ratio limit was not known at that time.) This increase in transformer ratio is at the expense of gradient unless a very small beam hole is used, and in that case beam stability is a major concern. A wakeatron with a transformer ratio of 10 and a gradient of 80 MeV/m has been discussed (52), and computer simulations are being used to study this concept in detail. In the future experimental work is planned at the advanced accelerator test facility at Argonne National Laboratory.

The switched power accelerator (53) is related closely to the wakefield transformer as illustrated in Figure 4. Instead of a drive beam, conductors are mounted between the disks of the transformer. These conductors are charged to a high voltage and then switched to ground resulting in an electrical pulse converging on the center. The transformer action of the radial transmission line increases the voltage substantially above the charging voltage. The switch is the key element, and a number of ideas including a laser/photocathode switch, a high pressure gas switch, and solid state switches have been discussed (54).

The laser/photocathode switches are being studied experimentally and with simulations. The goal of the experiments is a rugged cathode capable of high current density and with quantum efficiency of order 1%. Simulation results show that in a simple geometry about 10% of the stored energy before switching is converted to accelerating field energy (54). Azimuthal nonuniformity of the pulse caused by variation of the switch timing or efficiency would deflect the beam, and the sensitivity of the pulse to such variation is being measured with large scale models. In addition, for a large transformer ratio the switched power accelerator has a small beam hole. As in the case of the wakefield transformer this will lead to strong wakefield effects. With all of these aspects of the switched power linac under active investigation, in the near future it should be possible to evaluate the promise of this idea.

## PLASMA ACCELERATORS

Plasma accelerators offer the prospect of accelerating gradients in excess of 1 GeV/m; typical parameters are given in Table 1. In these accelerators a plasma oscillation with a longitudinal, accelerating field is produced; particles from an external source are injected into the plasma and accelerated. Two concepts which have been discussed widely, the plasma beatwave accelerator (55,56) and the plasma wakefield accelerator (44, 57), differ in the mechanism producing the plasma oscillation. The wakefield accelerator will be discussed first.

Table 1 Parameters for plasma accelerators from R. D. Ruth and P. Chen (58). [ ] indicate chosen parameters, and the other parameters are derived. The reference has a complete discussion.

| Parameter | Plasma beatwave accelerator ( $CO_2$ laser) | | Plasma wakefield accelerator | |
|---|---|---|---|---|
| $\omega$ ($sec^{-1}$) | [$1.78 \times 10^{14}$] | [$1.78 \times 10^{14}$] | - | - |
| N | - | - | [$5 \times 10^{10}$] | [$5 \times 10^{10}$] |
| $\gamma_i$ | - | - | [430] | [2040] |
| $\omega_p$ ($sec^{-1}$) | $5.7 \times 10^{12}$ | $2.7 \times 10^{12}$ | $4.4 \times 10^{12}$ | $4.4 \times 10^{12}$ |
| $n_0$ ($cm^{-3}$) | $1 \times 10^{16}$ | $2.2 \times 10^{15}$ | $6.0 \times 10^{15}$ | $6.0 \times 10^{15}$ |
| L (m) | [0.1] | [1.0] | [0.1] | [1.0] |
| $\alpha$[a] | [0.25] | [0.25] | 0.25 | 0.11 |
| $\delta$ | [$5\pi/16$] | [$5\pi/16$] | 0.042 | 0.018 |
| $\omega_p\tau$ | [1000] | [1000] | - | - |
| $\langle eE_z \rangle$ (GeV/m) | 2.0 | 0.94 | [2.0] | [0.94] |
| $R/(2\pi\ k_p)$ | 1.25 | 1.82 | [1.25] | [1.82] |
| R (mm) | 0.41 | 1.3 | 0.54 | 0.78 |
| $W\tau$ (J) | 11 | 240 | - | - |
| $N\gamma_i m_e c^2$ (J) | - | - | 1.8 | 8.4 |

[a] All symbols except $\alpha$ are defined in the text. $\alpha = n(r=0)/n_0 - 1$ where n(r) is the plasma density in Equation 9.

Maxwell's equations together with fluid equations describing the plasma are solved for a charged particle beam traveling in a plasma. While the complete solution should be non-perturbative and include relativistic motion of the plasma electrons, the perturbation solution for a non-relativistic plasma (44) gives insight into the basic phenomena. Assuming a driving beam of N particles in a disk with radial density distribution $\chi(r)$

$$n_b = N\,\chi(r)\,\delta(\,z - v_b t\,) \qquad 8.$$

the plasma density behind the beam ($z < v_b t$) is

$$n(r) = n_0 + k\,N\,\chi(r)\,\sin(\,k\,z - \omega_p t\,) \qquad 9.$$

where $n_0$ is the unperturbed density, $\omega_p$ ( = $(4\pi e^2 n_0/m_e)^{1/2}$ in cgs units) is the plasma frequency and $k = \omega_p/v_b$.

The electrostatic potential produced by the perturbation is calculated using Poisson's equation. When $\chi(r)$ is a parabolic distribution of radius R with $kR \gg 1$, the longitudinal and radial electric fields for $r \ll R$ are (44)

$$E_z = -\frac{8\,e\,N}{R^2}\left\{1 - \frac{r^2}{R^2}\right\}\cos(\,k\,z - \omega_p t\,)\,,$$

and 10.

$$E_r = \frac{16\,e\,N}{R^2}\left\{\frac{r}{k\,R^2}\right\}\sin(\,k\,z - \omega_p t\,)\,.$$

Features of this solution are (58):

1. The density perturbation is a static ($v_{group} = 0$) oscillation at the plasma frequency.
2. The number of particles, N, and the radius of the driving beam, R, determine the accelerating gradient.
3. For the chosen driving beam profile, $E_z$ depends on r; as a result the accelerated beam has an rms fractional energy spread of approximately $0.47(b/R)^2$ where b is the accelerated beam radius.
4. The useful phase region is between $\pi/2$ and $\pi$ where the fields are accelerating and focusing.
5. The phase velocity is $v_b$. Over a length L where the driving beam energy changes from $\gamma_i$ to $\gamma_f$ there is a phase slippage (44)

$$\delta = \frac{\omega_p\,L}{2\,\gamma_i\,\gamma_f\,c} \qquad 11.$$

between the beams. This limits the length of an acceleration stage.
6. The transformer ratio equals two (a consequence of assuming a disk in Equation 8); for a larger ratio the bunch must have an extended, non-symmetrical shape.

The driven beam also produces a wakefield and, therefore, loses some energy to the plasma. The net energy change is the increase from acceleration minus this energy loss. The maximum efficiency for the transfer of energy from the plasma to the beam is approximately $(b/R)^2$ which is about twice the energy spread (58). The accelerated beam

radius, b, is a function of the focusing and the beam emittance. The emittance is determined by particle physics, and the focusing strength and gradient are related. Using these relationships the efficiency is found to be proportional to $\epsilon_i(\omega_p/N\gamma)^{1/2}$. Is it possible to have simultaneously a high efficiency, a small energy spread, a small emittance, and a high gradient? The relationships between these quantities are dependent on $\chi(r)$, the driving beam radial profile (58). For $\chi(r)$ equal to a constant the efficiency can be increased without increasing the energy spread, but the emittance cannot be reduced sufficiently without increasing the plasma frequency (58)and the accompanying emittance blow-up due to multiple Coulomb scattering (59). While the importance of the driving beam radial profile is clear, to date there has not been a satisfactory positive answer to the question posed above.

The gradient, focusing strength, efficiency, and transformer ratio depend on the intensity and density distribution of the driving beam; this beam must be generated and propagated stably through the plasma. With the development of photoemitters combined with rapid acceleration, beams of the intensity needed may be feasible shortly, but the problems of control and manipulation of the radial and longitudinal distributions have not been considered in detail (60). Beam stability is being studied with theory and simulations. The conclusions are: an ultrashort, relativistic beam can be longitudinally stable until it has lost more than 70% of its energy to the plasma (61), transverse instabilities can be controlled with the transverse plasma temperature (61), and self-focusing could make control of the radial profile difficult, particularly for the long driving bunches needed for a high transformer ratio (62). There has been progress in understanding, but more work is needed.

In the beatwave accelerator the driving beam is replaced by two laser beams differing in frequency by $\omega_p$ (55,56). A single-frequency, plane wave cannot cause a net drift along the direction of propagation, but with two frequencies there is a modulation of the wave amplitude which results in a net force called the ponderamotive force. The plasma density perturbation grows linearly during the laser pulse, but can saturate due to secondary plasma modes (63) or relativistic effects (64). In the linear regime the density and the electric fields (for one particular $\chi(r)$) at the end of the pulse are given by Equations 9 and 10 with the replacement (58)

$$\frac{W\,\omega_p^2\,\tau}{4\,\omega^2\,m_e c^2} \rightarrow N \qquad 12.$$

The plasma frequency, the spot radius, and the laser pulse length ($\tau$), power (W), and average frequency ($\omega$) determine the gradient and focusing strength. With the laser pulse short enough to prevent exciting plasma modes other than the beatwave and the restriction that saturation be avoided, a rough rule-of-thumb is $\langle E_z(V/cm)\rangle_{max} \sim (n_0(cm^{-3}))^{1/2}$.

The length of an acceleration section can be limited by physical optics, phase slippage, or pump depletion (loss of laser energy to the

plasma). At low laser power the spot size is diffraction limited, and the section length should be $R^2\omega/c$, twice the Rayleigh length, for optimum use of the laser. At higher power a laser self-focuses in the plasma (65,66), and in simulations a single-frequency, self-focused laser beam is stable when its radius is of order $c/\omega_p$ (61). Self-focusing in the beatwave system is being examined; these studies should include the feasibility of varying the radial distribution for good efficiency.

The beatwave propagates with a phase velocity equal to the velocity of an electron with $\gamma_p = \omega/\omega_p$ (55); the phase slippage is given by Equation 11 with $\gamma_i = \gamma_f = \gamma_p$. Increasing $\gamma_p$ increases the section length and the energy gain per section but decreases the gradient. Pump depletion is not a limit for the beatwave accelerator (67), but the surfatron, which avoids phase slippage (68), is limited by pump depletion to section lengths roughly equal to those of the beatwave accelerator.

The dominant factor in the overall efficiency of the beatwave accelerator is the laser efficiency. At 10 $\mu$m wavelength a $CO_2$ laser can be used, and as discussed in conjunction with near-field accelerators, the short pulse efficiency of this laser is poor. Efficiencies of 7-10% are possible with KrF lasers, but these lasers are non-storage lasers with a pump time of 100 to 1000 nsec and an upper state lifetime of 5 nsec (41). Therefore, energy must be extracted throughout the pump period, and the short pulse efficiency is not good. NdYag lasers are capable of short pulses, but these lasers run at a low repetition rate. At the present time a laser appropriate for a very high energy collider is not available.

The possible gradient of a plasma accelerator is unmatched by any other novel accelerator concept. Can this potential be realized? It is too early to answer definitively (69). Efficiency and control are factors outside the model above and to a significant degree outside the realm of simulations. In both accelerators efficiency is related to the driving beam profile, and crucial information about self-focusing and the stability of the profile is missing. The plasma and driving beam must be controlled to the degree required by the small focal spots; the solution of this problem depends on experimentation to give guiding tolerances and technological advances.

The first plasma wakefield experiments are to begin shortly at Argonne National Laboratory; these experiments are being performed in collaboration with the University of Wisconsin and the University of California, Los Angeles. The goals are the observation of plasma waves driven by an electron beam and acceleration of particles by those waves (70).

In the first successful observation of the beatwave, a $CO_2$ laser emitting light at 10.6 $\mu$m and 9.6 $\mu$m excited a 2 mm long hydrogen plasma of density $n_0 \sim 10^{17}$ cm$^{-3}$ (71). The beatwave was diagnosed using Thomson scattering of ruby laser light. From the data it was concluded that the accelerating electric field was between 0.3 GeV/m and 1 GeV/m and that the plasma density modulation was greater than 3%. In this experiment the beatwave saturated due to coupling to secondary electrostatic modes (63). These secondary modes are associated with a

density ripple of the plasma ions and can be avoided with a laser pulse sufficiently short that the ions cannot move during the pulse (63).

The next goals of this group are the demonstration of acceleration of injected electrons and a study of interactions between these particles and the beatwave. To this end they are building a short pulse length laser to eliminate the saturation due to mode coupling, a small linear accelerator serving as the electron source, and a spectrometer for measuring energy changes. The experimental work with this system is beginning (72).

Beatwaves have also been inferred in a second experiment from the acceleration of injected particles (73). This experiment also used a $CO_2$ laser emitting at 9.6 $\mu$m and 10.6 $\mu$m, and both dry air and hydrogen gas were used. Typical plasma densities were 1 x $10^{17}$ $cm^{-3}$. Electrons from a laser illuminated Al target were injected into the plasma, and the preliminary results are that electrons injected at 0.6 Mev were accelerated to over 2 MeV in a 2 mm long plasma. This corresponds to a gradient of over 0.7 GeV/m.

A third experiment designed to observe beatwaves excited by 1 $\mu$m wavelength laser was unsuccessful because of a coincidental overlap with a rotational Raman spectrum line in $N_2$ (74). Time limitations have prevented repeating the experiment. An unanticipated outcome of the experiment was the observation of uniform plasmas produced by multiphoton ionization. To produce the beatwave the laser frequency difference must match the plasma frequency, and the production of uniform plasmas has been a potential practical barrier. Multiphoton ionization is a promising direction.

These experimental results are an encouraging beginning.

COLLECTIVE IMPLOSION ACCELERATOR

The "collective implosion accelerator" (75), shown schematically in Figure 5, exploits the large electrostatic fields produced by an intense, relativistic beam traveling in a low density gas. The electron charging beam ionizes the gas, and the ionization electrons are ejected from the beam. Ion density builds up at a rate proportional to the beam and gas densities and can be controlled with the gas density. The beam has a sharp trailing end and leaves behind itself an ion column wake.

The energy loss of the charging beam goes into electrostatic field energy and kinetic energy flux of electrons hitting the wall. The ratio of electrostatic field energy to energy loss is $f_e/2$ where $f_e$ is the fractional neutralization, $f_e$ = (ion line charge density at the tail of the beam)/(electron beam line charge density). For a typical set of parameters (an electron beam with a current of 10 kA, a pulse length of 50 nsec, and a gas density between $10^{13}$ and $10^{14}$ $cm^{-3}$) the deceleration rate is 20 keV/m, $f_e \sim 0.5$, and the electrostatic field energy is one-half the energy loss.

A picosecond laser pulse and the beam being accelerated follow the charging pulse. Before the ion column can disperse, the laser photoionizes a region of gas of large radial extent. The photoelectrons flow towards the ion column producing an accelerating field with a gradient of several hundred MeV/m. The ion dispersal time is of the order of 1 nsec. In addition to fixing the laser pulse delay, it specifies the sharpness of the electron beam tail; this together with

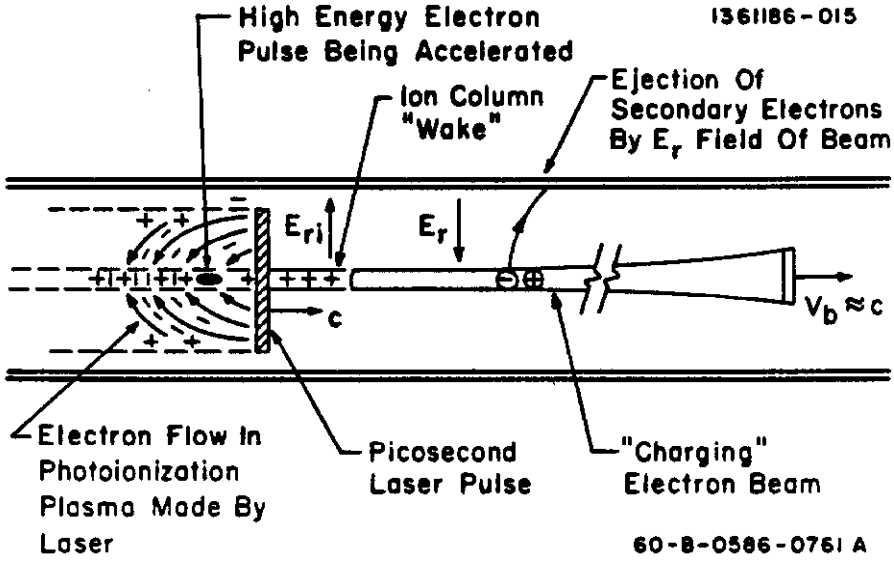


Figure 5: Schematic of the collective implosion accelerator concept (75). (Reprinted with permission of R. Briggs)

the rate at which the tail disperses fix the length of an acceleration section. Sections can be several hundred meters long before the tail needs to resharpened.

Additional simplifying features are: a preceding laser pulse can guide the charging beam (76), the charging beam is self focused (77), the picosecond laser pulse energy requirements are modest, and the inrush of electrons is focusing as well as accelerating. A disadvantage for linear colliders is that positron acceleration is not "natural", although a later phase of the plasma oscillation may be suitable. Overall, this accelerator concept combines a high gradient, a long section length, a high efficiency, and simplicity.

## SUMMARY AND CONCLUSION

Advanced accelerator concepts and their application to high energy physics have been reviewed. While the concepts selected do not make up an all-inclusive list, they are those receiving substantial attention in the accelerator community. To be cost effective for particle physics, small emittance beam and high acceleration efficiency are required. This is having a strong impact and is a stringent criterion for evaluation.

Experiments aimed at proving essential features are in progress or beginning soon. These experiments include the FEL power source, the wakefield transformer, the switched power accelerator, the beatwave accelerator, and the plasma wakefield accelerator. In addition, computer simulations are exploring issues related to using these concepts in complete accelerator systems.

Concepts which look promising in the proof-of-principle and simulation stages will be ready for detailed engineering. Prototype

design to develop this engineering will play an increasingly important role in meeting the challenge of $e^+e^-$ collisions at very high energies.

ACKNOWLEDGEMENTS

Papers by Perry Wilson (6), Wolfgang Schnell (34), and Ron Ruth and Pisin Chen (58) have been important to my understanding of advanced accelerator concepts. Chan Joshi reviewed the section on plasma accelerators. This paper was written at Fermilab which is operated by Universities Research Association, Inc under contract with the United States Department of Energy. Work at Cornell is supported in part by the National Science Foundation.

LITERATURE CITED

1. Superconducting Super Collider Conceptual Design, SSC-SR-2020(1986)
2. Tigner, M. Nuovo Cimento 37:1228-31(1965)
3. Amaldi, U. Phys. Lett. B61:313-15(1976)
4. SLC Design Handbook, Stanford Lin. Accel. Cntr.(1984)
5. Palmer, R. B. SLAC-PUB-3678, SLAC(1985)
6. Wilson, P. B. SLAC-PUB-3674, SLAC(1985). An earlier version which contains some errors is Wilson, P. B. AIP Conf. Proc. 130:560-97(1985)
7. Hollebeek, R. Nucl. Instrum. Methods 184:333-47(1981)
8. Fawley, W. M., Lee, E. P. UCID-18584, Lawrence Livermore Laboratory(1980)
9. Bassetti. M., Gygi-Hanney, M. LEP Note 221, CERN(1980)
10. Himel, T., Siegrist, J. AIP Conf. Proc. 130:602-8(1985)
11. Palmer, R. B. SLAC-PUB-3688, SLAC(1985)
12. Chen, P. SLAC-PUB-3823, SLAC(1985)
13. Brown, K. L., Servranckx, R. V. AIP Conf. Proc. 127:62-138(1985)
14. Bane, K. L. F. IEEE Trans. Nucl. Sci. NS-32:2389-91(1985)
15. Balakin, V. et al, Proc. 12th Int. Conf. on High Energy Accel., pp. 119(1983)
16. Sundelin, R. M. IEEE Trans. Nucl. Sci. NS-32:3570-73(1985)
17. Kneisel, P. AIP Conf. Proc. 156:in press
18. Peil, H. IEEE Trans. Nucl. Sci. NS-32:3565-69(1985)
19. Sundelin, R. M. CLNS-85/709, Cornell(1985)
20. Amaldi, U. et al, CERN/EF 86-8, CERN(1986)
21. Schnell, W. AIP Conf. Proc. 156:in press
22. Hopkins, D. B., Kuenning, R. W. IEEE Trans. Nucl. Sci. NS-32:3476-80(1985)
23. Lee, T. G. et al, SLAC-PUB-3619, SLAC(1985)
24. Chodorow, M. AIP Conf. Proc. 156:in press
25. Granatstein, V. L. et al, IEEE Trans. Nucl. Sci. NS-32:2957-59(1985)
26. Sinclair, C. AIP Conf. Proc. 156:in press
27. Yoshioka, M. AIP Conf. Proc. 156:in press
28. Farkas, Z. D. SLAC-PUB-3694, SLAC(1985)
29. Sessler, A. M. AIP Conf. Proc. 91:154-59(1982)
30. Birx, D. L. et al, IEEE Trans. Nucl. Sci. NS-32:2743-47(1985)
31. Orzechowski, T. J. et al, IEEE J. Quant. Electron. QE-21:831-44(1985)
32. Orzechowski, T. J. et al, Phys. Rev. Lett. 57:2172-75(1986)
33. Wurtele, J. AIP Conf. Proc. 156:in press
34. Schnell, W. CERN-LEP-RF/86-14, CERN(1986)

35. Marks, R. LBL-20918/UC-34A, Lawrence Berkeley Lab.(1985)
36. Amaldi, U., Pellegrini, C. CERN CLIC Note 16, CERN(1986)
37. Palmer, R. B. Part. Accel. 11:81-90(1980)
38. Kroll, N. AIP Conf. Proc. 130:253-70(1985)
39. Palmer, R. B. AIP Conf. Proc. 156:in press
40. Slater, J. AIP Conf. Proc. 130:505-17(1985)
41. Lowenthal, D., Slater, J. AIP Conf. Proc. 130:518-43(1985)
42. Fernow, R. AIP Conf. Proc. 156:in press
43. Palmer, R. B. AIP Conf. Proc. 156:in press
44. Ruth, R. D. et al, Part. Accel. 17:171-89(1985)
45. Voss, G.-A, Weiland, T. DESY M82-10, DESY(1982).
46. Voss, G.-A., Weiland, T. DESY 82-074, DESY(1982)
47. Weiland, T., Willeke, F. Proc. 12th Int. Conf. on High Energy Accelerators, pp 457(1983)
48. Weiland, T. IEEE Trans. Nucl. Sci., NS-32:3471-75(1985)
49. Decker, F.-J. AIP Conf. Proc. 156:in press
50. Ruggiero, A. G. AIP Conf. Proc. 130:458-74(1985)
51. Perevedentsev, E. A.,Skrinsky, A. N. Proc. of 6th All-Union Conf. on Charged Particle Accel., pp 272(1978)
52. Ruggiero, A. G. AIP Conf. Proc. 156:in press
53. Willis, W. AIP Conf. Proc. 130:421-34(1985)
54. Aronson, S. AIP Conf. Proc. 156:in press
55. Tajima, T., Dawson, J. M. Phys. Rev. Lett. 43:267-70(1979)
56. Joshi, C. et al, Nature 311:525-29(1984)
57. Chen, P. et al, Phys. Rev. Lett. 54:693-96(1985)
58. Ruth, R. D., Chen, P. SLAC-PUB-3906, SLAC(1986)
59. Montague, B. W.,Schnell, W. AIP Conf. Proc. 130:146-55(1985)
60. Fraser, J. S. et al, AIP Conf. Proc. 130:598-601(1985)
61. Bingham, R. AIP Conf. Proc. 156:in press
62. Katsouleas, T. AIP Conf. Proc. 156:in press
63. Darrow, C. et al, Phys. Rev. Lett. 56:2629-32(1986)
64. Rosenbluth, M. N., Liu, C. S. Phys. Rev. Lett. 29:701-5(1972)
65. Max, C. E. et al, Phys. Rev. Lett. 33:209-12(1974)
66. Forslund, D. W. et al, Phys. Rev. Lett. 54:558-61(1985)
67. Horton, W., Tajima, T. AIP Conf. Proc. 130:179-84(1985)
68. Katsouleas, T., Dawson, J. M. Phys. Rev. Lett. 51:392-95(1983)
69. Lawson, J. D. AIP Conf. Proc. 130:120-29(1985)
70. Rosenzweig, J. AIP Conf. Proc. 156:in press
71. Clayton, C. E. et al, Phys. Rev. Lett. 54:2343-50(1985)
72. Joshi, C. AIP Conf. Proc. 156:in press
73. Martin, F. et al, AIP Conf. Proc. 156:in press
74. Evans, R. G. et al, , AIP Conf. Proc. 156:in press
75. Briggs, R. J. Phys. Rev. Lett. 54:2588-91(1985)
76. Martin, W. E. et al, Phys. Rev. Lett. 54:685-88(1985)
77. Struve, K. W. et al, Proc. of the 5th Int. Conf. on High Power Part. Beams, pp 408 (1984)